

# Critical role of electronic correlations in determining crystal structure of transition metal compounds

Nicola Lanatà,<sup>1,\*</sup> Tsung-Han Lee,<sup>1,2,†</sup> Yong-Xin Yao,<sup>3,‡</sup> Vlada Stevanović,<sup>4,§</sup> and Vladimir Dobrosavljević<sup>1,¶</sup>

<sup>1</sup>*Department of Physics and National High Magnetic Field Laboratory, Florida State University, Tallahassee, FL 32310*

<sup>2</sup>*Department of Physics and Astronomy and Center for Condensed Matter Theory, Rutgers University, Piscataway, NJ 088548019*

<sup>3</sup>*Ames Laboratory-U.S. DOE and Department of Physics and Astronomy, Iowa State University, Ames, Iowa 50011*

<sup>4</sup>*Colorado School of Mines and National Renewable Energy Laboratory, Golden, Colorado 80401*

The choice that a solid system "makes" when adopting a crystal structure (stable or metastable) is ultimately governed by the interactions between electrons forming chemical bonds. By analyzing 6 prototypical binary transition-metal compounds we demonstrate here that the orbitally-selective strong  $d$ -electron correlations influence dramatically the behavior of the energy as a function of the spatial arrangements of the atoms. Remarkably, we find that the main qualitative features of this complex behavior can be traced back to simple electrostatics, i.e., to the fact that the strong  $d$ -electron correlations influence substantially the charge transfer mechanism, which, in turn, controls the electrostatic interactions. This result advances our understanding of the influence of strong correlations on the crystal structure, opens a new avenue for extending structure prediction methodologies to strongly correlated materials, and paves the way for predicting and studying metastability and polymorphism in these systems.

Predicting the ground-state structure of crystalline materials, initially thought to be an unsolvable problem, became an active area of research with the advent of efficient numerical implementation of computational total energy methods. Various approaches to exploring potential energy surface of solids (PES) from first principles (ab-initio thermodynamics) have been developed [1–3], leading to exciting discoveries such as superconducting dense hydrogen sulfide [4], new and intriguing forms of matter at elevated pressures [5], new functional materials [6–8], and other. Beyond the ground-state structures, efforts in exploiting polymorphism and extending structure prediction and materials by design strategies to metastable systems have also been pursued [9–12]. Describing accurately the PES was proven essential also in the efforts to predict from first principles new thermodynamically-stable topological insulators [13, 14] and Weyl-Kondo semimetals [15].

The space of strongly correlated electron systems, on the other hand, represents a virtually untapped territory for finding new materials exhibiting potentially ground-breaking physical properties. However, exploring the PES of these materials (usually  $d$ - or  $f$ -electron systems) poses significant challenges. This includes both the "choice" of the ground state structure, and the energy ordering of different PES local minima. The fact that strong electron correlations can influence the ground-state crystal structure has been demonstrated previously. For example, including correlations at an appropriate level of theory (Random Phase Approximation and Quantum Monte Carlo) was shown to be critical in reproducing the known rocksalt ground state structure of MnO [16–18]. Contrary to experiments, correlation-deficient approaches such as the classic approximations to density functional theory (DFT) [19, 20] would suggest zincblende or wurtzite structure, both featuring tetrahedrally coordinated atoms, to be lower in energy than the octahedrally coordinated rocksalt. However, the general physical mechanism through which electron correlations influence relative energies of different crystal structures remains elusive, and a systematic investigation of the role of correlations in determining the thermodynamically-stable crystal structure of transition metal compounds is presently missing.

In this paper we investigate the influence of strong electronic correlations present in  $d$ -transition metal compounds on the "choice" of the ground-state crystal structure of these systems. The main findings of our work are the following: (1) The strong electron correlations influence dramatically many important features of the PES in  $d$ -electron materials, such as the energy ordering of different polymorphs and the thermodynamically stable crystal structure. (2) Available theories describing the strong electron correlations beyond a mean-field single-particle picture, see, e.g., Refs. [21–28], provide us with effective tools for simulation-based structure-prediction studies of  $d$ -electron materials. (3) The main physical mechanism underlying the interplay between strong electron correlations and crystal structure in transition metal compounds — especially Mott insulators — is charge transfer, which governs the electrostatic interactions, that, in turn, play a decisive role in determining the ground-state structure.

\* lanata@magnet.fsu.edu; Contributed equally to this work

† tl596@physics.rutgers.edu; Contributed equally to this work

‡ ykent@iastate.edu

§ vstevano@mines.edu

¶ vlad@magnet.fsu.edu

The claims above are demonstrated here by studying 6 transition metal binary oxides and chalcogenides (CrO, MnO, FeO, CoO, CoS and CoSe) in 4 common crystal structure types shown in Fig.1 (rocksalt, NiAs-type, zincblende and wurtzite). This particular selection of crystal structures covers both the change in local coordination of the atoms and in the long range order, because it combines octahedral coordination with cubic symmetry (rocksalt), octahedral coordination with hexagonal symmetry (NiAs-type), tetrahedral coordination with cubic symmetry (zincblende) and tetrahedral coordination with hexagonal symmetry (wurtzite). Furthermore, the selected set includes the ground state structure for all studied systems. By employing a combination of local density approximation (LDA) [29] and the rotationally-invariant slave-boson (RISB) theory [28, 30, 31], which includes electron correlations beyond the single particle picture [24, 25, 27, 28, 30, 32], we were able to reproduce the experimentally known ground state structure of all compounds, as well as to uncover dominant physical mechanism by which strong correlations influence the energy ordering of different crystal structures.

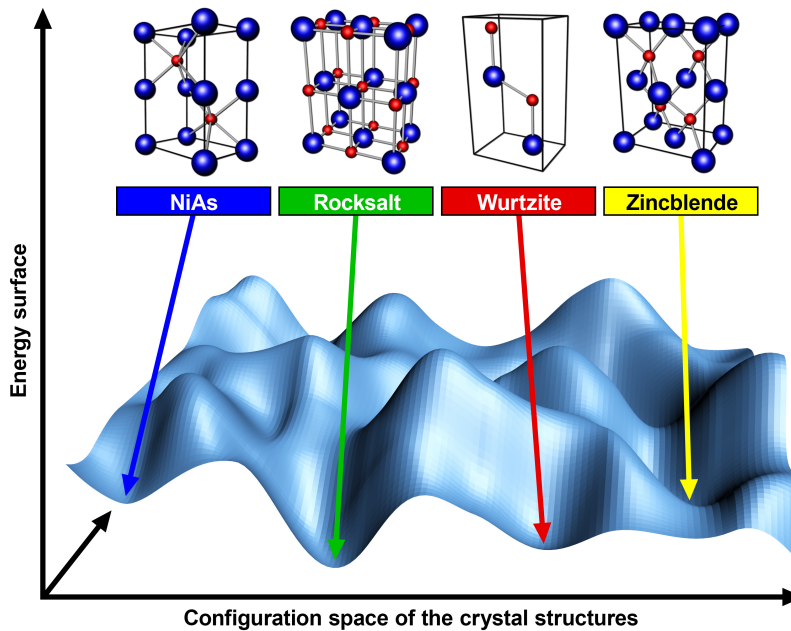


FIG. 1: Representation of generic energy profile as a function of the crystal configuration. Crystal structures considered in this work: NiAs-type, rocksalt, wurtzite, and zincblende.

## RESULTS

We have performed LDA, LDA+U [33] and LDA+RISB ground-state calculations of CrO, MnO, FeO, CoO, CoS and CoSe in 4 different crystal structures (rocksalt, NiAs-type, zincblende and wurtzite, see Fig. 1). The LDA+RISB calculations have been performed assuming a Hund's coupling constant strength  $J = 0.9 eV$  and scanning different values of Hubbard interaction strength  $U$ . Since all of these transition-metal compounds are paramagnetic at room temperature, the LDA+RISB simulations were performed assuming from the onset paramagnetic solutions.

In Fig. 2 is provided a bird's eye view of the main properties of the materials considered, inherent in their zero-temperature thermodynamically stable phase, i.e.: (1) the crystal configuration, (2) the equilibrium density, and (3) whether the system is a metal or an insulator. The theoretical results (triangles) are shown in comparison with the experiments (circles). The reported experimental data were obtained from Refs. [34–39]. The crystal structures are color coded by blue, green, red, yellow, for NiAs-type, rocksalt, wurtzite, and zincblende, respectively. The insulating phases are indicated by half-filled symbols, while the metallic phases are indicated by fully filled symbols.

From the experimental data we observe that all of the oxides considered favor the rocksalt structure, while the thermodynamically stable lattice configuration of CoS and CoSe is NiAs-type. All of the materials have a metallic ground state except MnO, FeO and CoO, which are Mott insulators.

As mentioned in the introduction, LDA fails to reproduce the experimental crystal structure (rocksalt) for all of the oxides. The method is also unable to capture the fact that MnO, FeO and CoO are insulators, and the predicted equilibrium volumes are generally inaccurate. Inclusion of spin polarization (ordering) at the level of

LDA+U or (GGA+U) straightens out the limitations of unpolarized LDA only in part. In particular, as shown in the Supplemental Material, the spin polarized GGA+U suggests different ground state structures of both CoS and CoSe depending on the value of  $U$ , never reproducing the experimentally known NiAs structure as the lowest energy one. The lowest energy structure changes from the rocksalt derived ( $U = 0 eV$ ) to zincblende ( $U = 6 eV$ ) and wurtzite ( $U = 12 eV$ ). Furthermore calculated equilibrium volumes are very different from the experimental ones. Hence, the experimentally observed change in the long-range order from the rocksalt to NiAs-type structure, that preserves octahedral coordination of atoms and occurs as the anion is replaced from CoO to CoS and CoSe, is overall poorly described by spin polarized GGA+U (or LDA+U). These results follow from an exhaustive enumeration of different spin configurations constructed on all symmetry inequivalent supercells with up to four formula units (approximately 700 calculations for both CoS and CoSe). The spin polarized GGA+U calculations were performed following the approach described in Ref. [40], which employs PAW treatment of valence electrons [41] and the Perdew-Burke-Ernzerhof (PBE) functional form for the exchange-correlation functional within the generalized gradient approximation to DFT [42], as implemented in the VASP code [43]. These results constitute unequivocal evidence of the fact that the strong electron correlations influence substantially the behavior of both the electronic structure and the total energy of these materials.

Remarkably, the LDA+RISB theory provides results in very good quantitative agreement with the experiments for all 6 transition metal binary oxides and chalcogenides considered, simultaneously. The simulations are particularly accurate for  $U = 13 eV$ . In fact, for this value of the Hubbard interaction strength, the method captures, at the same time, all of the physical properties examined, including the crystal structure and the insulating nature of MnO, FeO and CoO. Furthermore, the experimental equilibrium volumes of all materials are reproduced within 4% error. We note that the method captures the correct crystal structure of all materials also for  $U = 8 eV$ , although the overall accuracy of the results is not as satisfactory as for  $U = 13 eV$ . In particular, the equilibrium volume of FeO and CoO is underestimated for this value of  $U$ . The reason why varying the value of  $U$  influences considerably the equilibrium volume for these 2 materials is that the MIT of these 2 systems, which occurs at  $U \lesssim 13 eV$ , is first order. Consequently, the equilibrium volume evolves discontinuously at the critical point [44, 45]. Note that the values of the MIT critical  $U$  of FeO and CoO reported above are likely overestimated (this is a well-known systematic limitation of the RISB approximation).

These results indicate clearly that taking into account the strong electron correlations beyond the single-particle picture, e.g., utilizing the LDA+RISB approach, results in a remarkably effective tool for structure-prediction work of  $d$ -electron materials.

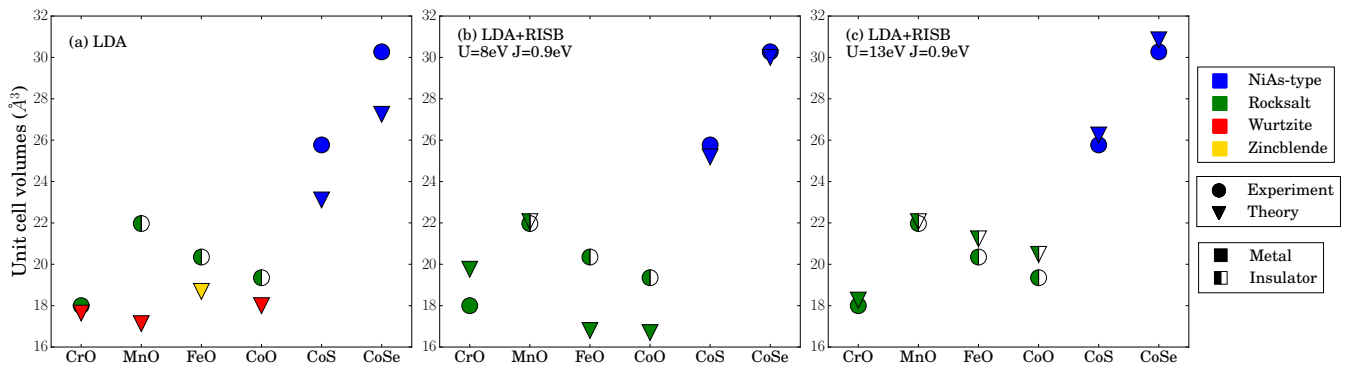


FIG. 2: Theoretical (triangles) unit cell volumes and crystal structures in comparison with the experiments (circles). The colors, blue, green, red, and yellow, correspond to NiAs-type, rocksalt, wurtzite, and zincblende structures, respectively. The metallic and insulating solution are labeled by filled and half-filled symbols, respectively.

In order to investigate in further detail the influence on the crystal structure of the strong  $d$ -electron correlations, and assess its relevance for the prediction of new polymorphs, it is also interesting to inspect the energy profiles of the thermodynamically unstable crystal configurations. For illustration purposes, the behavior of the theoretical total energy as a function of the volume is shown in Fig. 3 only for CoS and MnO, both in LDA and in LDA+RISB. The analysis of the other materials is reported in the Supplemental Material.

Interestingly, the RISB correction modifies dramatically the LDA energy order of the crystal structures, both for CoS (which is a metal) and MnO (which is a Mott insulator). We note also that the LDA+RISB relative energies between the different crystal structures of both MnO and CoS, evaluated at their respective experimental equilibrium volumes, are considerably larger with respect to the Néel temperature of the materials examined, that are all paramagnetic at

room temperature. In particular, the energy difference between the octahedrally coordinated configurations (Rocksalt and NiAs-type) and the tetrahedrally coordinated configurations (Wurtzite and Zincblende) is of the order of  $\sim 1$  eV for both of these materials.

The critical role of the strong electron correlations in determining the crystal structure is well exemplified by the calculations of MnO displayed in panel (d) of Fig. 3. In fact, MnO is a Mott insulator in the octahedrally coordinated structures, while it is a metal in the tetrahedrally coordinated structures. As shown in the Supplemental Material, the same behavior is observed in FeO and CoO, which (at their respective experimental equilibrium volumes) are also Mott insulators in their thermodynamically stable crystal configuration, while they are metals in the tetrahedrally coordinated structures.

These results indicate clearly that computing the behavior of the PES requires to take into account the subtle competing mechanisms underlying the strongly-correlated regime around the Mott transition — which can only be accomplished by many-body techniques able to take into account the strong electron correlations beyond a mean-field single-particle picture, such as DMFT and the RISB. In this respect, we note also that the interplay between crystal structure and  $d$ -electron correlations in the materials examined here is considerably more complex with respect to  $f$ -electron systems such as elemental Pr and Pu, where the RISB correction to the total energy was shown to be very similar for all phases [27].

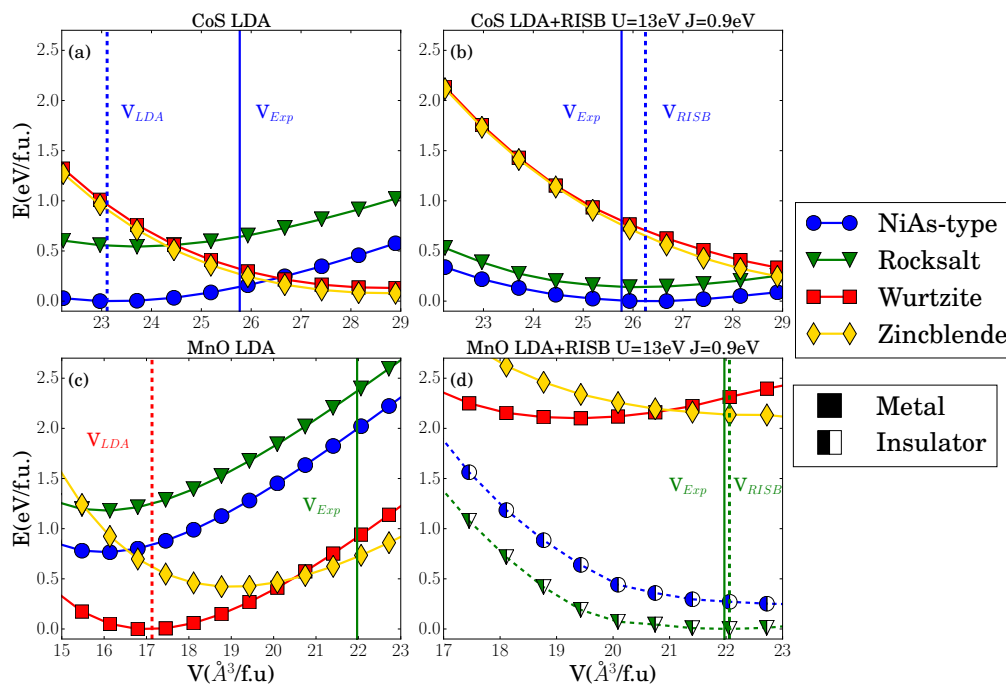


FIG. 3: LDA and LDA+RISB behaviour of the energy as a function of the volume for CoS (panels a,b) and MnO (panels c,d). The blue circle, green triangle, red square, and yellow diamond curves correspond to NiAs-type, rocksalt, wurtzite, and zincblende structures, respectively. The experimental equilibrium volumes for each compounds are marked by vertical solid lines, while the theoretical equilibrium volumes are marked by in dashed lines.

It is also interesting that turning on the  $d$ -electron Hubbard interaction has a qualitatively distinct effect on the relative energies between different crystal structures with respect to increasing the volume. In fact, for all of the materials considered, the LDA Wurtzite and Zincblende energies tend to become smaller than the Rocksalt and NiAs-type energies at larger volumes. Instead, turning on the interaction parameters ( $U, J$ ) has the opposite effect, i.e., it favors energetically the Rocksalt and NiAs-type structures. This consideration forces upon us the conclusion that the observed pronounced physical effects of the strong electron correlations on the behaviour of the total energy, which are accounted for by the LDA+RISB theory, are inherently "orbitally-selective"; in the sense that their influence on the crystal structure can not be simply traced back into a uniform renormalization of the bandwidth, as one might naively expect. As we are going to show, in fact, one of the main physical effects at play is charge transfer, which is a multi-orbital phenomenon decisively influenced by the strong electron correlations.

In order to investigate the connection between Mott physics and the energy order of the crystal structures, it is insightful to take a step back and analyze the energy-ordering problem from the point of view of a simple classic

point-ion electrostatic (PIE) model. The PIE model and the Madelung energy were successful in explaining the structure and the order-disorder phenomena in spinels [46, 47] as well as in non-isovalent perovskite alloys [48]. Here we employ the PIE model and Ewald summation described in Ref. [46], and evaluate the Madelung energies at the experimental equilibrium volumes, using as inputs the theoretical local  $d$ -electron occupations  $n_d$  reported in Table I. The point charges used to compute the Madelung energy are: (a) the transition metal sites are assumed to carry a positive charge equal to the total number of valence electrons minus the value of  $n_d$ , and (b) the anion sites are assumed to have a negative charge such as to make the system charge-neutral.

TABLE I: LDA and LDA+RISB  $d$ -electron occupations  $n_d$  computed at the experimental equilibrium volumes.

	NiAs-type		Rocksalt		Wurtzite		Zincblende	
	LDA	LDA+RISB	LDA	LDA+RISB	LDA	LDA+RISB	LDA	LDA+RISB
CrO	4.31	4.27	4.35	4.25	4.2	4.14	4.2	4.14
MnO	5.33	5	5.25	5	5.08	5.06	5.16	5.13
FeO	6.38	6	6.34	6	6.2	6.17	6.22	6.2
CoO	7.43	7	7.42	7	7.24	7.21	7.27	7.22
CoS	7.45	7.45	7.48	7.49	7.52	7.55	7.52	7.54
CoSe	7.52	7.51	7.52	7.51	7.57	7.6	7.52	7.51

Interestingly, the values of  $n_d$  are considerably influenced by the strong  $d$ -electron correlations, especially for the Mott insulating phases of MnO, FeO and CoO, which are realized in the NiAs-type and Rocksalt crystal structures. For these materials, we find that the simple PIE electrostatic model supplemented by the LDA+RISB occupations is sufficient to capture the correct LDA+RISB energy order between the different crystal structures at their respective experimental volumes, while this is not the case if the LDA occupations are used, see Fig. 4. This analysis enables us to prove that the tendency of electron correlations to favor energetically the Rocksalt and NiAs-type structures is a consequence of Mott physics and electrostatics. In fact, the key mechanism at play is that the metallic phases (which are tetrahedrally coordinated) display smaller charge transfer from the cation to the anion with respect to the Mott insulators (which are octahedrally coordinated). Note that, not surprisingly, the PIE model is unable to capture the energy order of the metallic systems CrO, CoS and CoSe (not shown), as the  $d$  electrons retain a significant mixed-valence character in these systems, and the covalent effects are very important.

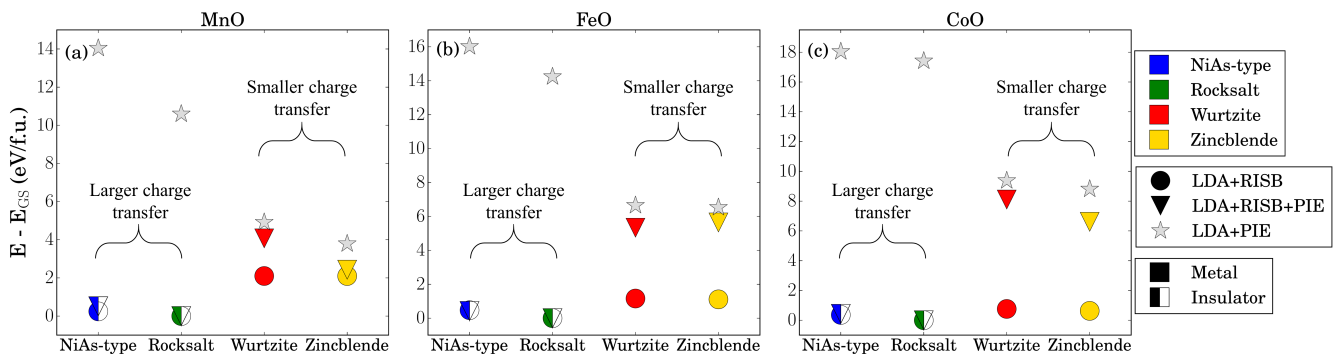


FIG. 4: Energy differences between different crystal structures, computed within LDA+RISB and the PIE model supplemented by the LDA+RISB  $d$  occupations (LDA+RISB+PIE) and the LDA  $d$  occupations (LDA+PIE). The results are shown for the Mott insulators MnO, FeO and CoO, and are computed at their respective experimental equilibrium volumes. The Rocksalt LDA+RISB+PIE and LDA+RISB energies are both conventionally assumed to be 0 in all materials considered.

In summary, the main reason why the strong  $d$ -electron correlations affect dramatically the crystal structure of these materials is that they influence substantially the charge transfer mechanism, which, in turn, controls the electrostatic interactions. This mechanism is particularly transparent in the Mott insulators (MnO, FeO and CoO), where the role of the strong electron correlations is magnified. As we have shown, the energy order is considerably influenced by the

$d$ -electron correlations also in the metallic systems examined. However, the qualitative features of the chemical bonds in these metals can not be captured by electrostatics alone, as the covalent effects are also very important. In this respect, it is also interesting to note that for metallic systems (CrO, CoS and CoSe) the energy differences between crystal structures are much smaller than in the case of Mott insulators, implying a more subtle balance between electrostatic and covalent effects — which is accurately captured by a proper treatment of strong correlations.

## CONCLUSIONS

We have analyzed theoretically the “choice” of the ground state structure of 6 transition-metal binary oxides and chalcogenides among 4 different crystal structures, utilizing LDA in combination with the rotationally-invariant slave-boson (RISB) theory, finding very good quantitative agreement with the experiments. These simulations demonstrated that the subtle competing mechanisms underlying the strongly-correlated regime influence dramatically the behaviour of the PES — and, in particular, the energy order between different crystal configurations — in all of the transition metal compound considered.

Remarkably, we found that the main qualitative features inherent in the influence of the strong electron correlations on the crystal structure can be understood in terms of a simple electrostatic model, based on the sole knowledge of the  $d$ -electron occupations. This analysis enabled us to demonstrate that one of the key physical effects which must be taken into account in order to predict the correct energy ordering of these materials is the variation of charge transfer induced by the strong  $d$ -electron correlations around the Mott point. On the other hand, as expected, electrostatics alone can not capture also the energy order of the metallic systems, where the  $d$  electrons retain a significant mixed-valence character, and the covalent effects are non-negligible.

These results indicate that simulation-based structure-prediction work of all transition-metal compounds (metals and insulators) requires theoretical tools able to describe, at the same time: (i) the details of the bands structure, and (ii) the  $d$ -electron correlations around the Mott transition — which influence substantially the electronic structure and, in particular, the charge-transfer mechanism in these materials. For this purpose, taking into account the strong electron correlations beyond single-particle mean-field schemes, such as LDA and LSDA+U, is an absolute necessity. In this respect, the LDA+RISB technique is particularly appealing, as it is both sufficiently accurate and computationally convenient to be applied to high-throughput computational materials design of this class of systems.

Another important conclusion arising from our study is that the typical energy differences between different crystal structures, which have been all computed assuming paramagnetic solutions from the onset, are generally much larger with respect energy scales characterizing magnetism in all of the materials considered (and most of the known transition metal oxides). This observation indicates that magnetic order has generally a negligible effect on the total energy with respect to the  $d$ -electron atomic scales originating the orbitally-selective correlations. This physical insight results also in an appealing simplification from the computational standpoint, as it suggests that it is possible to perform accurate structure-prediction work assuming from the onset paramagnetic solutions (as we did in the LDA+RISB calculations of the present work), i.e., without breaking translational invariance or time reversal symmetry.

## METHODS

The LDA and LDA+RISB calculations were performed utilizing the DFT code WIEN2k [49]. The LDA+RISB solver was implemented following Ref. [28]. The LAPW interface between WIEN2k and the RISB was implemented as described in Ref. [50], utilizing the fully-localized limit (FFL) double-counting functional [33]. All calculation were performed setting 50000  $k$ -points and  $RKmax = 8$ .

## ACKNOWLEDGEMENTS

TH, VD, and NL were partially supported by the NSF grant DMR-1410132 and the National High Magnetic Field Laboratory. YY was supported by the U.S. Department of energy, Office of Science, Basic Energy Sciences, as a part of the Computational Materials Science Program. VS acknowledges support of the Center for the Next Generation of Materials by Design, an Energy Frontier Research Center funded by the U.S. Department of Energy, Office of Science, Basic Energy Sciences. The research was performed using computational resources sponsored by the Department of Energy’s Office of Energy Efficiency and Renewable Energy and located at the National Renewable Energy Laboratory. We thank Kevin John for providing us with Fig. 1.

## AUTHOR CONTRIBUTIONS

V.S. and V.D. initiated the project. All the authors contributed to the analysis and the interpretation of the results, and to writing the manuscript. N.L. and T.-H.L. equally contributed to this work. T.-H.L., N.L. and Y.-X.Y. performed the LDA+RISB calculations, while V.S. performed the DFT+U calculations.

## COMPETING FINANCIAL INTERESTS

The authors declare no competing financial interests.

- 
- [1] Woodley, S. M. & Catlow, R. Crystal structure prediction from first principles. *Nat Mater* **7**, 937–946 (2008).
- [2] Oganov, A. *Modern methods of crystal structure prediction* (Wiley-VCH John Wiley distributor, Weinheim Chichester, 2010).
- [3] Atahan-Evrenk, S. & Aspuru-Guzik, A. *Prediction and calculation of crystal structures: methods and applications* (Springer, Cham Switzerland, 2014).
- [4] Li, Y., Hao, J., Liu, H., Li, Y. & Ma, Y. The metallization and superconductivity of dense hydrogen sulfide. *J. of Chem. Phys.* **140**, 174712 (2014).
- [5] Ma, Y. *et al.* Transparent dense sodium. *Nature* 182–185.
- [6] Hautier, G. *et al.* Phosphates as lithium-ion battery cathodes: An evaluation based on high-throughput ab initio calculations. *Chemistry of Materials* **23**, 3495–3508 (2011).
- [7] Peng, H., Ndione, P. F., Ginley, D. S., Zakutayev, A. & Lany, S. Design of semiconducting tetrahedral  $Mn_{1-x}Zn_xO$  alloys and their application to solar water splitting. *Phys. Rev. X* **5**, 021016 (2015).
- [8] Jain, A., Shin, Y. & Persson, K. A. Computational predictions of energy materials using density functional theory. *Nature Reviews Materials* 15004.
- [9] Botti, S., Flores-Livas, J. A., Amsler, M., Goedecker, S. & Marques, M. A. L. Low-energy silicon allotropes with strong absorption in the visible for photovoltaic applications. *Phys. Rev. B* **86**, 121204 (2012).
- [10] Huan, T. D. *et al.* Low-energy polymeric phases of alانات. *Phys. Rev. Lett.* **110**, 135502 (2013).
- [11] Stevanović, V. Sampling polymorphs of ionic solids using random superlattices. *Phys. Rev. Lett.* **116**, 075503 (2016).
- [12] Jones, E. B. & Stevanović, V. Polymorphism in elemental silicon: Probabilistic interpretation of the realizability of metastable structures. *Phys. Rev. B* **96**, 184101 (2017).
- [13] Trimarchi, G., Zhang, X., Freeman, A. J. & Zunger, A. Structurally unstable  $A^{iii}B_{2}O_3$  perovskites are predicted to be topological insulators but their stable structural forms are trivial band insulators. *Phys. Rev. B* **90**, 161111 (2014).
- [14] Zhang, X., Abdalla, L. B., Liu, Q. & Zunger, A. The enabling electronic motif for topological insulation in  $ABO_3$  perovskites. *Advanced Functional Materials* **27**, 1701266–n/a (2017). 1701266.
- [15] X.-Y. Feng, J. D., H. Zhong & Si, Q. Dirac-kondo semimetals and topological kondo insulators in the dilute carrier limit. unpublished (2016). cond-mat/1605.02380.
- [16] Schrön, A., Rödl, C. & Bechstedt, F. Energetic stability and magnetic properties of MnO in the rocksalt, wurtzite, and zinc-blende structures: Influence of exchange and correlation. *Phys. Rev. B* **82**, 165109 (2010).
- [17] Peng, H. & Lany, S. Polymorphic energy ordering of MgO, ZnO, GaN, and MnO within the random phase approximation. *Phys. Rev. B* **87**, 174113 (2013).
- [18] Schiller, J. A., Wagner, L. K. & Ertekin, E. Phase stability and properties of manganese oxide polymorphs: Assessment and insights from diffusion monte carlo. *Phys. Rev. B* **92**, 235209 (2015).
- [19] Hohenberg, P. & Kohn, W. Inhomogeneous electron gas. *Phys. Rev.* **136**, B864 (1964).
- [20] Kohn, W. & Sham, L. J. Self-consistent equations including exchange and correlation effects. *Phys. Rev.* **140**, A1133 (1965).
- [21] Kotliar, G. *et al.* Electronic structure calculations with dynamical mean-field theory. *Rev. Mod. Phys.* **78**, 865 (2006).
- [22] Georges, A., Kotliar, G., Krauth, W. & Rozenberg, M. J. Dynamical mean-field theory of strongly correlated fermion systems and the limit of infinite dimensions. *Rev. Mod. Phys.* **68**, 13 (1996).
- [23] Anisimov, V. & Izyumov, Y. *Electronic Structure of Strongly Correlated Materials* (Springer, 2010).
- [24] Deng, X.-Y., Wang, L., Dai, X. & Fang, Z. Local density approximation combined with Gutzwiller method for correlated electron systems: Formalism and applications. *Phys. Rev. B* **79**, 075114 (2009).
- [25] Ho, K. M., Schmalian, J. & Wang, C. Z. Gutzwiller density functional theory for correlated electron systems. *Phys. Rev. B* **77**, 073101 (2008).
- [26] Lanatà, N., Barone, P. & Fabrizio, M. Fermi-surface evolution across the magnetic phase transition in the Kondo lattice model. *Phys. Rev. B* **78**, 155127 (2008).
- [27] Lanatà, N., Yao, Y.-X., Wang, C.-Z., Ho, K.-M. & Kotliar, G. Phase diagram and electronic structure of praseodymium and plutonium. *Phys. Rev. X* **5**, 011008 (2015).

- [28] Lanatà, N., Yao, Y.-X., Deng, X., Dobrosavljević, V. & Kotliar, G. Slave boson theory of orbital differentiation with crystal field effects: Application to  $\text{UO}_2$ . *Phys. Rev. Lett.* **118**, 126401 (2017).
- [29] Gunnarsson, O. & Lundqvist, B. I. Exchange and correlation in atoms, molecules, and solids by the spin-density-functional formalism. *Phys. Rev. B* **13**, 4274 (1976).
- [30] Li, T., Wölfle, P. & Hirschfeld, P. J. Spin-rotation-invariant slave-boson approach to the Hubbard model. *Phys. Rev. B* **40**, 6817 (1989).
- [31] Lechermann, F., Georges, A., Kotliar, G. & Parcollet, O. Rotationally invariant slave-boson formalism and momentum dependence of the quasiparticle weight. *Phys. Rev. B* **76**, 155102 (2007).
- [32] Piefke, C. & Lechermann, F. LDA + slave-boson approach to the correlated electronic structure of the metamagnetic bilayer ruthenate  $\text{Sr}_3\text{Ru}_2\text{O}_7$ . *Phys. Stat. Sol. (B)* **248**, 2269 (2011).
- [33] Anisimov, V. I., Aryasetiawan, F. & Lichtenstein, A. I. First-principles calculations of the electronic structure and spectra of strongly correlated systems: the LDA+U method. *J. Phys. Condens. Matter* **9**, 767 (1997).
- [34] Dufek, V., Petrů, F. & Brožek, V. Über sauerstoff-haltige verbindungen vom strukturtyp b1 der ersten vier übergangsmetalle. *Monatshefte für Chemie und verwandte Teile anderer Wissenschaften* **98**, 2424–2430 (1967).
- [35] Radler, M. *et al.* The defect structures of  $\text{Mn}_{1-x}\text{O}$ . *Journal of Physics and Chemistry of Solids* **53**, 141 – 154 (1992).
- [36] Crisan, O. & Crisan, A. Phase transformation and exchange bias effects in mechanically alloyed Fe/magnetite powders. *Journal of Alloys and Compounds* **509**, 6522 – 6527 (2011).
- [37] Jauch, W., Reehuis, M., Bleif, H. J., Kubanek, F. & Pattison, P. Crystallographic symmetry and magnetic structure of  $\text{CoO}$ . *Phys. Rev. B* **64**, 052102 (2001).
- [38] Barthelemy, E. & Carcaly, C. Phase relations and ageing effects in  $\text{Fe}_{1-x}\text{Co}_x\text{S}$  system. *Journal of Solid State Chemistry* **66**, 191 – 203 (1987).
- [39] Dalal, V. K., Keer, H. & Biswas, A. Studies on some mixed chalcogenides. *Journal of Inorganic and Nuclear Chemistry* **33**, 2839 – 2845 (1971).
- [40] Stevanović, V., Lany, S., Zhang, X. & Zunger, A. Correcting density functional theory for accurate predictions of compound enthalpies of formation: Fitted elemental-phase reference energies. *Phys. Rev. B* **85**, 115104 (2012).
- [41] Blöchl, P. E. Projector augmented-wave method. *Phys. Rev. B* **50**, 17953–17979 (1994).
- [42] Perdew, J. P., Burke, K. & Ernzerhof, M. Generalized gradient approximation made simple. *Phys. Rev. Lett.* **77**, 3865–3868 (1996).
- [43] Kresse, G. & Furthmüller, J. Efficiency of ab-initio total energy calculations for metals and semiconductors using a plane-wave basis set. *Comput. Mater. Sci.* **6**, 15 (1996).
- [44] Huang, L., Wang, Y. & Dai, X. Pressure-driven orbital selective insulator-to-metal transition and spin-state crossover in cubic  $\text{CoO}$ . *Phys. Rev. B* **85**, 245110 (2012).
- [45] Kunes, J., Lukyanov, A. V., Anisimov, V. I., Scalettar, R. T. & Pickett, W. E. Collapse of magnetic moment drives the mott transition in  $\text{MnO}$ . *Nat Mater* 198–202.
- [46] Stevanović, V., d’Avezac, M. & Zunger, A. Simple point-ion electrostatic model explains the cation distribution in spinel oxides. *Phys. Rev. Lett.* **105**, 075501 (2010).
- [47] Stevanović, V., d’Avezac, M. & Zunger, A. Universal electrostatic origin of cation ordering in  $\text{A}_2\text{BO}_4$  spinel oxides. *Journal of the American Chemical Society* **133**, 11649–11654 (2011).
- [48] Bellaïche, L. & Vanderbilt, D. Electrostatic model of atomic ordering in complex perovskite alloys. *Phys. Rev. Lett.* **81**, 1318–1321 (1998).
- [49] Schwarz, K. & Blaha, P. Solid state calculations using WIEN2k. *Computational Materials Science* **28**, 259 – 273 (2003).
- [50] Haule, K., Yee, C.-H. & Kim, K. Dynamical mean-field theory within the full-potential methods: Electronic structure of  $\text{CeIrIn}_5$ ,  $\text{CeCoIn}_5$ , and  $\text{CeRhIn}_5$ . *Phys. Rev. B* **81**, 195107 (2010).



# Supplemental Materials: Critical role of electronic correlations in determining crystal structure of transition metal compounds

## I. LSDA+U ANALYSIS OF CoS AND CoSe

In Tables II and III are shown the spin polarized GGA+U total energies and volumes for CoS and CoSe in four different structure types (NiAs-type, Rocksalt, Zinblende, and Wurzite). Each total energy corresponds to the lowest energy spin configuration for the corresponding crystal structure at its respective relaxed volume. These results were obtained from an exhaustive enumeration of different spin configurations constructed on all symmetry inequivalent supercells with up to four formula units (approximately 700 spin polarized GGA+U calculations for both CoS and CoSe). The GGA+U calculations were performed following the approach described in Ref. [40], which employs PAW treatment of valent electrons [41] and the Perdew-Burke-Ernzerhof (PBE) form for the exchange-correlation functional within the generalized gradient approximation to DFT [42], as implemented in the VASP code [43]. Each total energy corresponds to the lowest energy spin configuration for that structure at the respective relaxed volume.

We observe that the lowest-energy spin state predicts an incorrect energy ordering of the different crystal structures for all values of  $U$ . For  $U = 0$ , GGA+U predicts that all solutions are metallic, and the NiAs-type (which is thermodynamically stable experimentally) has the highest energy. For  $U = 6$  the GGA+U lowest-energy structure becomes Zinblende (remains wrong), and, in addition, all solutions are insulators with volumes that are quite far from the experimental one. The results do not improve for  $U = 12$  eV, as the GGA+U lowest-energy structure becomes Wurtzite and also insulating. We point out also that the energy differences between the GGA+U lowest-energy structures and the NiAs-type structure are considerably large for all values of  $U$ . In particular, at  $U = 0$  we find about  $200\text{meV}/f.u.$  for CoS and about  $300\text{meV}/f.u.$  for CoSe. For larger values of  $U$ , the energy difference between Rocksalt and NiAs-type decreases, but the GGA+U energy minimum now becomes realized by the Zinblende and the Wurzite structures. Actually, for all values of  $U$  the energy preference is toward the tetrahedrally coordinated structures. Even in case of  $U = 0$ , for which the ground state is obtained by relaxing the initial rocksalt structure, the structural relaxations within the spin polarized GGA+U break the symmetry of the rocksalt structure and transform it to the tetrahedrally coordinated structures with  $Cm$  and  $P4/mnm$  space groups for CoS and CoSe, respectively. For  $U = 6$  eV and  $U = 12$  eV the rocksalt structure is stable. Therefore, the spin polarized GGA+U fails dramatically in reproducing known crystal structure and correct energy ordering in these systems.

These results demonstrate that the strong electron correlations influence substantially the behavior of both the electronic structure and the total energy of the correlated metals considered.

TABLE II: Spin polarized GGA+U total energies  $E_{tot}$  and volumes  $V$  for CoS in 4 different structure types (NiAs-type, Rocksalt, Zinblende, and Wurzite), computed at 3 different values of the Hubbard  $U$ . Each total energy corresponds to the lowest energy spin configuration for the corresponding crystal structure at its respective relaxed volume. The total energy is always referenced to the ground state structure for a given  $U$  value.

	$U = 0\text{ eV}$		$U = 6\text{ eV}$		$U = 12\text{ eV}$	
	$E_{tot}$ [eV/f.u.]	$V$ [eV/f.u.]	$E_{tot}$ [eV/f.u.]	$V$ [eV/f.u.]	$E_{tot}$ [eV/f.u.]	$V$ [eV/f.u.]
NiAs-type	0.164	24.92	0.216	32.16	0.179	33.09
Rocksalt	0.000	28.92	0.235	32.15	0.184	33.06
Wurzite	0.050	30.56	0.000	40.59	0.002	42.23
Zinblende	0.003	28.59	0.019	40.88	0.000	42.34

TABLE III: Spin polarized GGA+U total energies  $E_{tot}$  and volumes  $V$  for CoSe in 4 different structure types (NiAs-type, Rocksalt, Zincblende, and Wurtzite), computed at 3 different values of the Hubbard  $U$ . Each total energy corresponds to the lowest energy spin configuration for the corresponding crystal structure at its respective relaxed volume. The total energy is always referenced to the ground state structure for a given  $U$  value.

	$U = 0 eV$		$U = 6 eV$		$U = 12 eV$	
	$E_{tot}$ [eV/f.u.]	$V$ [eV/f.u.]	$E_{tot}$ [eV/f.u.]	$V$ [eV/f.u.]	$E_{tot}$ [eV/f.u.]	$V$ [eV/f.u.]
NiAs-type	0.283	29.36	0.189	37.34	0.198	38.68
Rocksalt	0.000	39.05	0.232	37.32	0.220	38.77
Wurtzite	0.376	36.56	0.000	47.58	0.000	49.42
Zincblende	0.311	33.36	0.016	47.84	0.001	49.54

## II. LDA+RISB ANALYSIS OF ENERGY ORDER FOR ALL STRUCTURES.

In Fig. 5 are shown the LDA+RISB total energy differences of CrO, MnO, FeO, CoO, CoS and CoSe computed for all of the crystal structures considered at the experimental equilibrium volumes realized at ambient conditions. The lowest energy of each material is conventionally considered 0. The metallic and insulating solution are labeled by filled and half-filled symbols, respectively.

As discussed in the main text, MnO, FeO and CoO are Mott insulators in the octahedrally coordinated structures (Rocksalt and NiAs-type), while they are metals in the tetrahedrally coordinated structures (Wurtzite and Zincblende).

We observe that the RISB correction modifies dramatically the LDA energy order of all systems. For the metallic materials (CrO, CoS and CoSe) the energy differences between crystal structures are much smaller than in the Mott insulators, implying a more subtle balance between electrostatic and covalent effects.

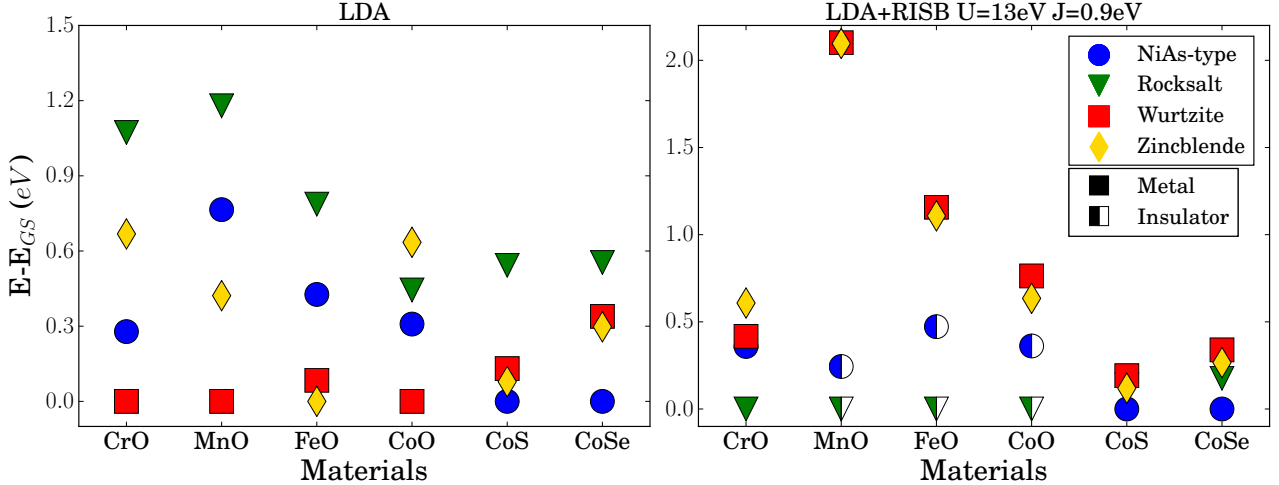


FIG. 5: Total energy differences of CrO, MnO, FeO, CoO, CoS and CoSe in all of the crystal structures considered at the respective equilibrium volumes at ambient conditions. The blue circle, green triangle, red square, and yellow diamond curves correspond to NiAs-type, rocksalt, wurtzite, and zincblende structures, respectively. The metallic and insulating solution are labeled by filled and half-filled symbols, respectively.